DALTON
FULL PAPER

Hydrogen-bonded neutral and anionic lamellar networks: Crystal structures of bis(*O*,*O*′,*O*″-hydroorotato)disilver(I) dihydrate, potassium hydroorotate and rubidium hydroorotate. *Ab initio* calculations on orotic acid and the hydroorotate anion †

Somer Bekiroglu and Olof Kristiansson *

Department of Chemistry, SLU, Box 7015, SE-750 07 Uppsala, Sweden.
E-mail: olof.kristiansson@kemi.slu.se

Received 13th November 2001, Accepted 23rd January 2002
First published as an Advance Article on the web 12th March 2002

The complex adducts of silver(I) (**1**), potassium(I) (**2**) and rubidium(I) (**3**) with the hydroorotate (2,6-dioxo-1,2,3,6-tetrahydropyrimidine-4-carboxylate) anion have been prepared, and their structures determined by X-ray diffraction. Crystals of bis(*O*,*O*′,*O*″-hydroorotato)disilver(I) dihydrate (**1**) consist of a polymeric structure which is based on bis(hydroorotato-*O*,*O*′) bridged dimers, analogous to those found in many O,O′-bridged silver carboxylates. Extensive hydrogen-bonding and secondary carbonyl-O ··· Ag interactions result in infinite, neutral sheets with an interplanar spacing of 3.085 Å. Crystals of **2** ($KC_5H_3N_2O_4$) consist of a lamellar structure with infinite anionic sheets parallel to the crystallographic (100) plane. The distance between two adjacent sheets is 3.417 Å and the K^+ cations are situated between the sheets with slightly distorted square antiprismatic geometries. Compound **3** ($RbC_5H_3N_2O_4$) is essentially isostructural with the potassium analogue with the interplanar spacing increased to 3.600 Å. *Ab initio* calculations on orotic acid and the hydroorotate anion were performed. The optimized geometries and harmonic vibrational frequencies were computed using density functional theory B3LYP/6-31G(d) model chemistry. ^{1}H and ^{13}C NMR chemical shifts were calculated at the HF/6-311++(2d,2p) and B3LYP/6-311++G(2d,2p) levels, and compared with experimental values.

Introduction

The multifunctionality of the hydroorotate, H_2L^-, and orotate, HL^{2-}, anions offer interesting possibilities in crystal engineering as a versatile ligand for supramolecular assemblies. Metal ion coordination may occur through the two N atoms of the pyrimidine ring as well as the two carbonyl oxygen atoms or the carboxylic group, which results in a multi-faceted coordination chemistry. The coordinated orotate anions exhibit a ligand surface with double or triple hydrogen-bonding capabilities, depending on the metal coordination mode, and has thus a potential to adopt several modes of interligand hydrogen bonding to allow the formation of extended, self-assembled structures. In this paper we present the crystal structures of silver(I) (**1**), potassium(I) (**2**) and rubidium(I) (**3**) with the hydroorotate anion. Extensive hydrogen-bonding and secondary carbonyl-O ··· Ag interactions result in infinite, neutral sheets for **1** and lamellar structures with infinite anionic sheets for **2** and **3**. *Ab initio* calculations on orotic acid and the hydroorotate anion were also employed to gain further insight in gas phase IR, NMR and geometrical properties.

Orotic acid, H_3L (see Scheme 1), acts as a diacid in aqueous solution, with the acidic function suggested to be located on the carboxylic group ($pK_{a1} = 2.09$) and on the N3 site ($pK_{a2} = 9.45$).[1] The monobasic form, hydroorotate, H_2L^-, appears to predominantly form complexes with coordination through the carboxyl oxygen atoms. With the Cu(I)[2] and Zn(II)[3] cations, a bidentate coordination is observed whereas UO_2(II) coordinates monodentately.[4] Compounds with the Zn(II)[5] and Mg(II)[6] cations, where the H_2L^- anion does not enter the inner coordination sphere of the cation have also been reported.

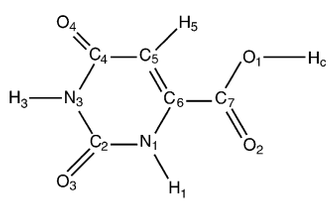

Scheme 1 Orotic acid (2,6-dioxo-1,2,3,6-tetrahydropyrimidine-4-carboxylic acid; uracil-6-carboxylic acid; vitamin B13; H_3L).

With the dibasic form HL^{2-}, the predominant coordination mode is a bidentate O2–N1 mode as observed for the Cu(II),[7,12] Ni(II),[8] Pt(II),[9,10] Pd(II),[11] Ir(I) and Rh(I)[12] cations. This coordination mode is also observed with Group 6 metal carbonyls.[13] In some cases, mixed coordination modes are observed where the orotate anion acts as a bridging ligand to form polymeric structures. In $[Mn_2[HL]_2(H_2O)_6]$, for example, polymeric chains result where the HL^{2-} anion links three manganese atoms *via* O2–N1, O1 and O4.[14] One rare example of N3 coordination is found in hexaamine bis(5-nitroorotato)tricopper(II) where tribasic L^{3-} ligands bridge two copper atoms *via* N1–O1 and N3 coordination.[15] Recently, a complex containing both H_2L^- and HL^{2-} has been structurally characterized, namely $[Fe_3(\mu_3\text{-}OH)(H_2L)_3(HL)_3]$.[16] The H_2L^- anion bridges two Fe(III) cations *via* the carboxylate group whereas HL^{2-} chelates one Fe(III) by the bidentate O2–N1 mode and is bonded to a second Fe(III) through the adjacent carbonyl oxygen atom. In short, the hydroorotate and orotate anions exhibit nine different

† Electronic supplementary information (ESI) available: energies and geometries of optimized structures (Table S1). Intramolecular geometry of orotic acid and the hydroorotate anion in the gas phase and crystalline surroundings (Table S2). Calculated and measured ^{1}H and ^{13}C chemical shifts for orotic acid and the hydroorotate anion (Table S3). Observed and calculated IR frequencies for selected vibrations of orotic acid and the hydroorotate anion (Table S4). See http://www.rsc.org/suppdata/dt/b1/b110386p/

 DOI: 10.1039/b110386p

coordination modes in the compounds so far crystallographically characterized.

The most interesting aspect of orotate chemistry is that the coordinated orotate anions exhibit a ligand surface with a double or triple hydrogen-bonding functionality, depending on the metal coordination mode. The common O2–N1 bidentate coordination, for example, results in a H-bond acceptor–donor–acceptor (ADA) motif which is potentially capable of forming hydrogen bonds with compounds possessing complementary DAD or DA motifs, such as 2,6-diaminopyridine or adenine, as demonstrated by Mingos and co-workers.[12] This molecular level recognition of organic molecules may have interesting implications in both pharmaceutical and materials chemistry, where the orotate or hydroorotate anions can be used as versatile synthons for the assembly of metal–organic supramolecular architectures.

In this paper, we wish to present the crystal structures of complexes between the monovalent cations Ag^+, K^+ and Rb^+ with the hydroorotate ligand. Silver carboxylates have been extensively studied and as a result a large number of structures have been published.[17] The dominating structural motif is based on eight-membered rings formed from O,O′-bridged dimers, bis(carboxylato)disilver(I). The dimers often form polymeric chains by bridging neighboring dimeric units with longer, secondary Ag–O bonds. We felt it would be of interest to investigate the structures resulting from these basic bis(carboxylato)disilver(I) units and the hydrogen-bonding capabilities of the hydroorotate anion, which may allow the polymeric chains to be linked into sheets. For comparison, due to the similar ionic radius of Ag^+ and K^+, the crystal structure of potassium hydroorotate has been determined. Moreover, to investigate the influence of a small increase in ionic radius upon the crystal organization, rubidium hydroorotate is also included in this study.

Ab initio calculations on orotic acid and the hydroorotate anion were performed with a two-fold objective. On the one hand, we wished to determine the geometry and electron distribution in the isolated orotic acid and hydroorotate anion for comparison with the geometries observed in crystalline surroundings so as to ascertain the effects of cations and hydrogen bonds. On the other, we wished to examine IR and NMR properties. The vibrational spectra of orotic acid and the hydroorotate anion are both relatively complex. Five contributions of relatively high intensity, namely the two carbonyl, the asymmetric and symmetric carboxylic and the C=C stretching vibrations, are found in the 1300–1600 cm^{-1} wavenumber region. Furthermore, these vibrations may be strongly coupled, and we found it worthwhile therefore to perform a vibrational analysis to assess the usefulness of these vibrations as probes for the bonding situations in hydroorotate and orotate complexes. Finally, calculated NMR properties were used mainly to clarify an ambiguity that existed in the assignment of the H1 and H3 proton signals.

Results and discussion

Bis(*O*,*O*′,*O*″-hydroorotato)disilver(I) dihydrate. Crystal structure

The crystal structure is based on bis-carboxylato bridged $Ag_2(C_5H_3N_2O_4)_2$ dimers (Fig. 1). The Ag–Ag distance is 2.8421(7) Å, a value in the range normally observed for silver carboxylates. The silver ions are coordinated to the carboxylic oxygen atoms O1 and O2 with distances of 2.190(3) and 2.196(3) Å, respectively, and to the carbonyl oxygen atom O4 from adjacent dimers with a significantly longer distance, 2.419(3) Å. The O1–Ag1–$O2^i$ and $Ag1^i$–Ag1–O4 angles are 164.29(10) and 163.45(8)°, giving the silver ion a distorted square planar geometry. The average deviation from the atoms defining the pyrimidine ring is 0.0064 Å, consistent with the pseudo-aromatic nature of the uracil ring. The O1–O2–Ag1–$Ag1^i$–$O1^i$–

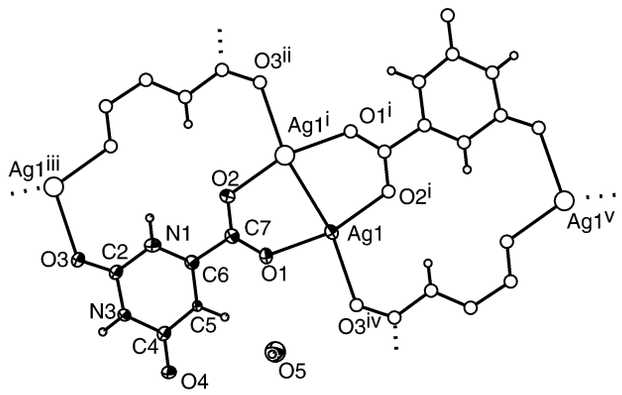

Fig. 1 View of bis(*O*,*O*′,*O*″-hydroorotato)disilver(I) dihydrate (**1**) with displacement ellipsoids drawn at the 50% probability level. Selected bond lengths (Å): Ag1–O1, 2.190(3); Ag1–$O2^i$, 2.196(3); Ag1–$O4^{ii}$, 2.419(3); Ag1–$Ag1^i$, 2.8421(7); O1–C7, 1.246(5); O2–C7, 1.256(5); O3–C2, 1.224(5); O4–C4 1.255(5). Selected bond angles (°): O1–Ag1–$O2^i$, 164.29(10); O1–Ag1–$O4^{ii}$, 106.71(10); O1–C7–O2, 127.6(4). Symmetry codes: (i) $-x, -y, -z$; (ii) $1-x, -1-y, -z$; (iii) $-x-1, -y-1, -z-1$; (iv) $x-1, y+1, z$; (v) $-x, -2-y, -1-z$.

$O2^i$ moiety is planar, with a mean deviation of 0.0049 Å, and the dihedral angle between this plane and the pyrimidine ring is 9.3°. This results in an overall average deviation from the plane of the extended chain of 0.1001 Å.

The $Ag_2(C_5H_3N_2O_4)_2$ units are linked *via* the Ag–O4 secondary bond and N–H ··· O hydrogen bonds (d(N–O) = 2.836(5) Å) to form 1-D chains (Fig. 2). Adjacent chains are linked by two N–H ··· O hydrogen bonds per orotate molecule, with the O–N distance equal to 2.853(5) Å, to form infinite 2-D sheets. The result is the lamellar structure shown in Fig. 3. The inter-planar distance between two sheets is 3.085 Å, a value exceptionally short compared to values in the range 3.29–3.71 Å observed in an investigation of π–π interactions in a number of pyrene and pyrene-like molecules,[18] or the value of 3.35 Å observed in graphite. However, adjacent sheets are displaced such that no appreciable contact between the hydroorotate ligands occurs. Instead, the hydroorotate ligands in one sheet are positioned over the Ag_2O_6 moieties in the adjacent sheet.

Two water molecules occupying the relatively large voids in the sheets complete the crystal structure. The water molecules form several hydrogen bonds but it was not possible to unambiguously determine the positions of the hydrogen atoms from the electron density maps, most probably due to disorder resulting from the many possibilities of hydrogen bonding environments as can be seen in Fig. 4. Each water molecule has two donor and three acceptor sites within hydrogen bonding range (d(O ··· O,N < 3.2 Å).

This structure presents a certain resemblance to those formed by the bis(3-aldoximepyridine)silver(I) cation with perchlorate or hexafluorophosphate counterions. These structures are linked by the oxime moiety in a similar way, O–H ··· N hydrogen bonds form chains which in turn are linked by C–H ··· O hydrogen bonds to form infinite cationic sheets.[19] Within these sheets, voids are found which are occupied by the counterions; similar to those of the present structure occupied by water molecules.

Potassium and rubidium hydroorotate. Crystal structures

Potassium hydroorotate forms a lamellar structure with infinite anionic sheets parallel to the crystallographic (100) plane. The distance between two adjacent sheets is 3.417 Å. The K^+ cations are situated between the sheets and have slightly distorted square antiprismatic geometries (Fig. 5). The square faces, belonging to adjacent anionic sheets, are situated 1.798 Å from the cations. The K1–O1 and K1–O3 distances are 2.736(6) and 2.871(5) Å, respectively. The hydroorotate ion lies on a mirror

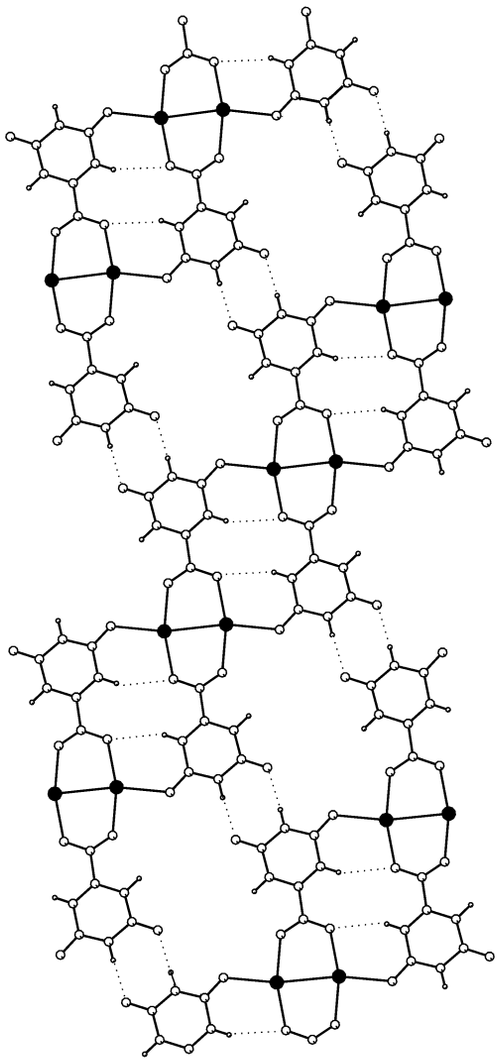

Fig. 2 Part of one of the hydrogen-bonded sheets of **1**. The water molecules are omitted for clarity. Solid circles = Ag.

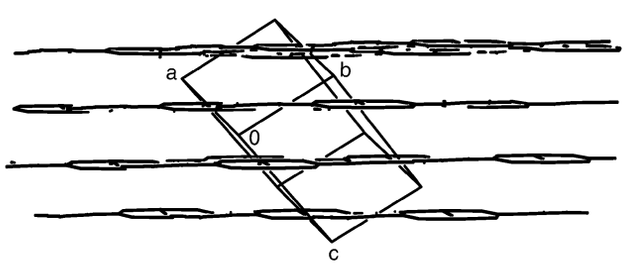

Fig. 3 View of the unit cell content of **1** showing the lamellar structure with an inter-planar spacing of 3.085 Å.

plane and is consequently strictly planar. A two-fold axis passes through the C7–C6–N3 atoms, which makes the C5 and N1 atoms indistinguishable. The C6–C5(N1) distance is 1.360(9) Å, as compared with C6–C5 and C6–N1 distances of 1.346(1) and 1.372(1) Å, respectively, in *e.g.* ammonium hydroorotate.[20] The hydroorotate anions act as μ_8 bridging ligands (Fig. 6). Each hydroorotate anion is linked to two others with four equivalent N(C)–H ··· O hydrogen bonds (d(N–O) = 3.132 Å) to form planar ribbons, as shown in Fig. 7. These ribbons are cross-linked by relatively weak, bifurcated hydrogen bonds between N3 and the carboxylate oxygen atoms. Adjacent sheets are held together by electrostatic forces between the negatively charged layers and the potassium ions but the relatively short inter-planar distance, 3.417 Å, suggests that aromatic π–π interactions also play an appreciable role in the non-bonded crystal organization.

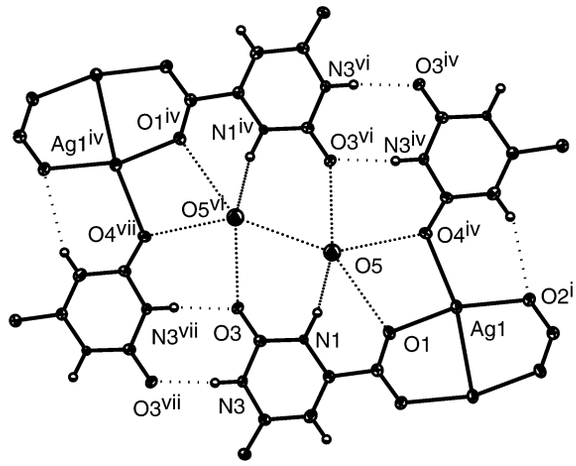

Fig. 4 View of the hydrogen-bonded network in **1**. Selected distances (Å): O5–O1, 3.010(5); O5–N1, 2.836(5); O5–O5^{iii}, 3.172(5); O5–O3^{iii}, 2.818(5); O5–O4^{iv}, 2.933(5); N3–O3, 2.853(5). Symmetry codes as in Fig. 1 and: (vi) $x - 1, -y - 1, -z - 1$; (vii) $x, -y - 2, -z - 1$.

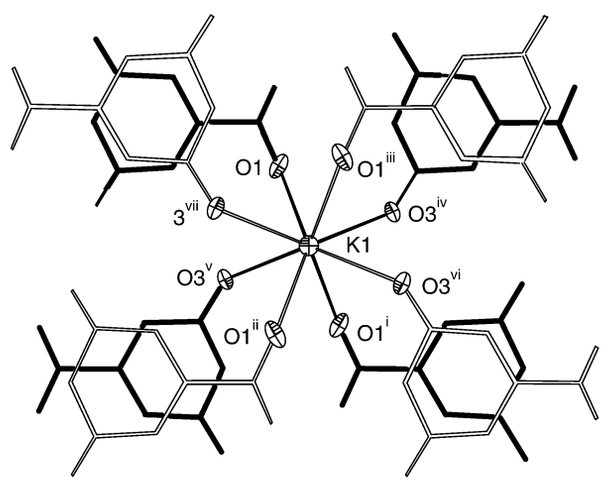

Fig. 5 View of potassium hydroorotate (**2**) showing the coordination of the K^+ cation. Selected bond lengths (Å): K1–O1, 2.736(6); K1–O3, 2.871(5). Symmetry codes: (i) $-x, 3/2 - y, z$; (ii) $x - 1/2, 1/2 + y, z$; (iii) $1/2 - x, 3/2 - y, -z$; (iv) $x - 1/2, y + 1/2, 1 + z$; (v) $1/2 - x, 3/2 - y, 1 - z$; (vi) $x, y, z + 1$; (vii) $-x, 1 - y, 1 - z$; (viii) $-x, 1 - y, -z$.

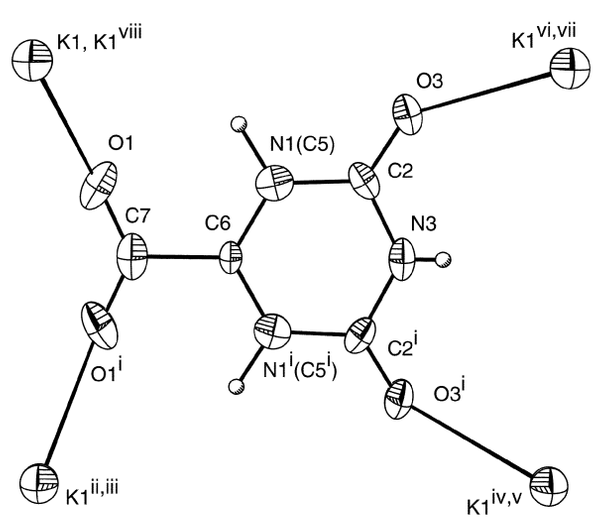

Fig. 6 Coordination of the hydroorotate anion in **2**. Each oxygen atom coordinates two K^+ cations, situated 1.798 Å above and below the plane defined by the hydroorotate anion. Selected distances (Å): K1–O1, 2.736(6); K1–O3, 2.871(5).

Rubidium hydroorotate is essentially isostructural with the potassium analogue. The larger ionic radius of Rb^+, 1.75 Å, compared to 1.65 Å for the octa-coordinated K^+ cation,[21]

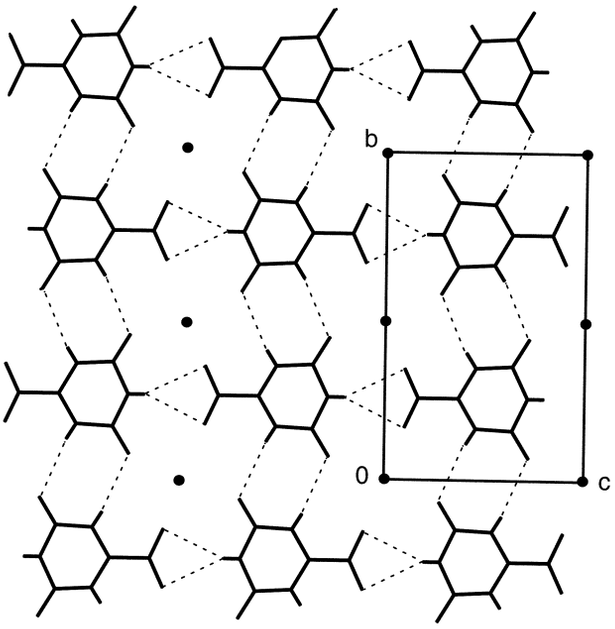

Fig. 7 View parallel to the (100) plane of the packing in the unit cell of **2**. The K^+ ions, shown as solid circles, are situated at $a = 0$ and 1/2 and the anionic sheets at $a = 1/4$ and 3/4.

causes the interplanar spacing to be increased by 0.183 Å to 3.600 Å. The *b*- and *c*-axes are increased by 0.197 Å to 12.762 Å and by 0.085 Å to 7.758 Å, respectively. This increase is mainly an effect of a lengthening of the N1–O3 and N3–O4 hydrogen bonds of 0.074 and 0.049 Å, respectively. The Rb–O distances are 2.862 (O1) and 2.995 (O2) Å and the approximately square faces of the cubic antiprism are 3.205 and 3.360 Å. The lower crystal interaction energy caused by the increased interplanar spacing and the decreased hydrogen bond strengths is reflected by an increased solubility of rubidium hydroorotate as compared to potassium hydroorotate. The solubilities are 0.039 and 0.013 mol dm^{-3}, for $RbC_4H_3O_4N_2$ and $KC_4H_3O_4N_2$, respectively, at 20 °C, in spite of the lower hydration enthalpy of Rb^+ compared to K^+.

To compare, lithium hydroorotate also crystallizes in a lamellar structure with the Li^+ ion tetrahedrally coordinated to three hydroorotate ligands *via* the O2, O3 and O4 oxygen atoms and to one solvate water molecule.[6] The distance between successive planes is 3.2 Å, with the Li^+ ions situated 0.53 Å from these planes. Adjacent sheets are similarly displaced, such that no appreciable contact between the hydroorotate ligands occurs. The crystal structure of potassium and rubidium hydroorotate presents certain similarities with that of ammonium hydroorotate monohydrate.[20] Also in this case planar ribbons are formed by N1–O4 hydrogen bonds (d(N–O) = 2.864(1) Å). The ribbons are, however, crosslinked by extensive hydrogen bonds with the ammonium ions and solvate water molecules.

Intramolecular geometry of orotic acid and the hydroorotate anion in the gas phase and in crystalline surroundings

The intramolecular geometry of orotic acid, as obtained by the density functional theory (DFT) method using the standard 6-31G(d) basis set and B3LYP hybrid functionals[22] as supplied in the Gaussian-98 program,[23] is given in Tables S1 and S2 (ESI). Of the two possible locations for the carboxylic proton, O1 and O2, in orotic acid, the O1 conformer is 6.0 kJ more stable and the results given below are calculated for this conformation. The molecule is strictly planar with bond distances as expected for this pseudo-aromatic system. However, the carboxylic group is significantly tilted towards N1–H1 with the C5–C6–C7 and N1–C6–C7 angles equal to 124.7 and 113.1°, respectively, *i.e.* the C6–C7 bond forms an angle of 172.3° with the line joining C6 and N3. This tilt is presumably an effect of the highly bent intramolecular hydrogen bond N1–H1 ⋯ O2 with an N1–O2 distance of 2.698 Å and an N1–H1–O2 angle of 101.6°. This interpretation is supported by the calculated vibrational spectrum where the N1–H1 stretching vibration is considerably down-shifted (3453 cm^{-1}) as compared to the N3–H3 stretching vibration (3620 cm^{-1}) where no hydrogen bond is present. This tilt toward the NH grouping is accompanied by an asymmetry of the C6–C7–O1 and C6–C7–O2 angles, which are 113.1 and 122.6°, respectively (Table S2, ESI). The fully optimized molecular structure is very similar to the structure obtained from X-ray diffraction of orotic acid monohydrate, including the tilt of the carboxylic group.[24] All distances within the ring are somewhat elongated in the crystal as compared with calculated values (0.01–0.04 Å). The C=O(carbonyl) distances are somewhat shortened and the C7–O1 and C7–O2 distances elongated by 0.037 and 0.017 Å, respectively, as a result of the intermolecular hydrogen bonds formed in the condensed phase.

Deprotonation of O1 to give the hydroorotate anion results in the expected changes of C7–O2 and C7–O1 from 1.214 and 1.343 to 1.244 and 1.261 Å, respectively, and an increase of the C6–C7 distance from 1.494 to 1.561 Å. A similar tilt of the carboxylic group as observed for orotic acid is apparent. Coordination to the monovalent cations NH_4^+, K^+, Rb^+ and Ag^+ only results in minor changes. The C=O(carboxylic) distances are changed less than 0.02 Å, suggesting a weak interaction between these cations and the hydroorotate ligand. Surprisingly, the largest change introduced by the cations is a decrease in the N3–C4 distance of 0.05 Å. Similar energies and geometries were also obtained from DFT calculations at a lower level of theory in the context of an investigation of the reaction mechanisms of the decarboxylation of orotic acid.[25]

Ab initio calculations at the HF/6-311G** level including the MP2 correlation energy of the two possible orotate anions, HL^{2-}, revealed that the conformer with the N3 site deprotonated is 29.8 kJ mol^{-1} more stable relative to the conformer with the N1 site deprotonated. This is presumably an effect of the stabilization of the former conformer by the intramolecular hydrogen bond formed between N1–H1 and O2. In aqueous solution, this difference in stability between the conformers will presumably be diminished since both H1 and H3 are stabilized by hydrogen bonds to water molecules in this situation.

NMR and IR spectroscopy

Calculated ^1H and ^{13}C chemical shifts of orotic acid and the hydroorotate anion are given in Table S3 (ESI). Two sets of NMR data were calculated at the HF/6-311++G(2d,2p) and B3LYP/6-311++G(2d,2p) levels. The experimental ^1H chemical shifts of hydroorotate, H_2L^-, are identical (11.24, 10.57 and 6.18 ppm) for saturated aqueous solutions of $M(H_2L)$ where M = NH_4^+, Li^+, Na^+, K^+, Cs^+ and Rb^+, implying either that these electrolytes are fully dissociated in aqueous solution or that monovalent cations coordinated to the carboxylic group have no effect on the charge distribution of the ring system.

The NMR chemical shifts calculated for orotic acid and the hydroorotate anion were used in the assignment of H1 and H3 shifts, which could not be distinguished by experimental means. The calculated H1 chemical shifts resulted in more upfield chemical shifts as compared to the ones of H3. Accordingly the experimental chemical shifts of H3 protons could be assigned to more downfield shifts following the same trend observed in calculated values. Interestingly, the chemical shift of the H5 proton was calculated to be 6.408, 6.050 with B3LYP and 6.250, 5.781 ppm with HF for orotic acid and orotate anion, respectively. These results actually have a very satisfactory accuracy and match with the experimental values ranging from 6.180 to 6.200 ppm for orotate anions in the presence of different counterions, and 6.223 ppm for orotic acid. This finding of the

calculations should indeed reflect a coincidence and be used routinely to make a relative comparison since the accuracy of chemical shift calculations for protons is known to be rather questionable.[26] Macroscopic factors, *i.e.* the behavior of individual molecules in a solution environment, also induce inaccuracies in NMR calculations, as well as in all theoretical studies excluding solvent effects. However, it was neither implicitly nor explicitly possible to perform these calculations in the presence of solvent. These calculations are also affected drastically by structural changes. For instance, the upfield shifted chemical shift of H1 in orotate anion originates from structural changes (0.282 Å shorter H ··· O distance, 0.01 Å longer N–H bond, 10° larger N–H ··· O angle) and electron distributions (the extra negative charge) with respect to orotic acid. Similarly in chemical shift calculations on H1 and H3 of orotic acid and orotate anions, the margin of error between the calculated and the experimental chemical shift values is rather large, giving *ca.* 4 ppm difference for orotate anion and stressing the more downfield shifted character of the H3 proton.

The vibrational spectra of orotic acid and the hydroorotate anion are both relatively complex. Five contributions of relatively high intensity, namely the two carbonyl, the asymmetric and symmetric carboxylic and the C=C stretching vibrations, are found in the 1300–1700 cm^{-1} wavenumber region. Furthermore, these vibrations may be strongly coupled, and we found it therefore worthwhile to perform a vibrational analysis to assess the usefulness of these vibrations as probes for the bonding situations in hydroorotate and orotate complexes. Vibrational frequencies in the harmonic approximation were computed with the same method and basis set as the geometry optimization. Calculated and observed frequencies for orotic acid and the hydroorotate anion for selected vibrations are given in Table S4 (ESI). During the course of this investigation, a vibrational analysis of orotic acid using isotopic substitutions for experimental spectra and DFT calculations using the Becke3P86/6-311G** basis set was reported.[27] The agreement between this and the present calculation is generally good even though some small discrepancies exist (Tables S4, ESI).

Conclusion

Bis(*O*,*O*′,*O*″-hydroorotato)disilver(I) dihydrate consists of a polymeric structure which is based on bis(hydroorotato-*O*,*O*′) bridged dimers, where extensive hydrogen-bonding and secondary carbonyl-O ··· Ag interactions result in infinite, neutral sheets with an interplanar spacing of 3.085 Å. Potassium- and rubidium-hydroorotate have lamellar structures with infinite anionic sheets. The cations are situated between the sheets with slightly distorted square antiprismatic geometries. The hydroorotate anion manifests its multifunctionality with two new coordination modes in addition to the nine different modes so far crystallographically characterized.

Experimental

Mikrokemi AB, Uppsala, Sweden, carried out microanalyses (C, H and N). Infrared spectra were recorded on a Perkin-Elmer 1711 FT-IR spectrometer in the 500–5000 cm^{-1} range as KBr pellets for crystalline samples. ^{1}H and ^{13}C NMR spectra were recorded on a Bruker DRX spectrometer operating at 400 MHz.

Synthesis

Bis(*O*,*O*′,*O*″-hydroorotato)disilver(I) dihydrate, 1. 1.62 g (10 mmol) Orotic acid monohydrate (Fluka p.a.) was added to 250 ml water containing 0.5611 g (10 mmol) KOH (Fluka, purum). To this suspension was added dropwise, while boiling and stirring, a solution containing 1.65 g $AgNO_3$ (10 mmol) (Merck, p.a.). A white precipitate formed immediately. After filtration X-ray quality crystals were obtained by slow cooling of the mother liquor. The two solids formed were identical as observed by superimposable IR spectra. The solubility in water is *ca.* 14 and 91 mg/100 cm^3 at 20 and 100 °C, respectively. Anal. found for **1**: C, 21.5; H, 1.1; N, 9.9. Calc. for $C_{10}H_6Ag_2N_4O_8$: C, 21.52; H, 1.08; N, 10.04%. IR (ν/cm^{-1}): 3482 (br, s), 3146 (s), 3105 (w), 3088 (m), 2988 (w), 1698 (vs), 1616 (m), 1491 (m), 1421 (w), 1377 (s), 1306 (w), 1224 (m), 1111 (w), 1007 (m), 922 (m), 890 (m), 870 (w), 809 (m), 773 (s), 761 (m), 641 (w), 591 (w), 546 (m). NMR (D_2O/ppm): 6.20 (s), 10.59 (s), 11.24 (s). UV λ/nm (ε/dm^3 mol^{-1} cm^{-1}): 278 (2.4×10^4), 206 (3.9×10^4), 198 (sh).

Potassium hydroorotate, 2. 1.62 g (10 mmol) Orotic acid monohydrate (Fluka p.a.) was added to 250 ml water containing 0.5611 g (10 mmol) KOH (Fluka, purum). A white precipitate formed immediately. After filtration X-ray quality crystals were obtained by slow cooling of the mother liquor. The two solids formed were identical as observed by superimposable IR spectra. The solubility in water is *ca.* 0.26 g/100 cm^3 at 20 °C. Anal. found for **2**: C, 31.1; H, 1.6; N, 14.3. Calc. for $C_5H_3KN_2O_4$: C, 30.92; H, 1.56; N, 14.43%. IR (ν/cm^{-1}): 3158 (s, br), 3108 (m), 3087 (m), 2988 (m), 2854 (w), 2746 (w), 1700 (vs), 1617 (m), 1492 (m), 1473 (w), 1459 (vw), 1420 (m), 1377 (s), 1306 (w), 1225 (m), 1112 (w), 1022 (w), 1005 (w), 921 (m), 891 (m), 810 (m), 772 (s), 762 (m), 641 (w), 591 (w), 546 (s). NMR (D_2O/ppm): 6.18 (s), 10.56 (s), 11.24 (s). UV λ/nm: 278, 296.

Rubidium hydroorotate, 3. 1.62 g (10 mmol) Orotic acid monohydrate (Fluka p.a.) was added to 250 ml water containing 0.5611 g (10 mmol) RbOH (Aldrich, purum). A white precipitate formed immediately. After filtration X-ray quality crystals were obtained by slow cooling of the mother liquor. The two solids formed were identical as observed by superimposable IR spectra. The solubility in water is *ca.* 0.94 g/100 cm^3 at 20 °C. Anal. found for **3**: C, 24.8; H, 1.3; N, 11.7. Calc. for $C_5H_3N_2O_4Rb$: C, 24.96; H, 1.26; N, 11.65%. IR (ν/cm^{-1}): 3210 (m), 3159 (m), 3107 (w), 3089 (w), 3001 (m), 2759 (m), 1944 (vw), 1811 (vw), 1698 (vs), 1621 (w), 1488 (m), 1458 (w), 1419 (w), 1378 (s), 1308 (w), 1220 (m), 1107 (w), 1020 (m), 919 (m), 887 (m), 809 (w), 773 (m), 639 (w), 588 (w), 544 (m), 434 (m). NMR (D_2O/ppm): 6.18 (s), 10.56 (s), 11.24 (s). UV λ/nm: 278, 296.

Crystallography

Data were collected using Mo-Kα radiation on a Bruker SMART platform equipped with a CCD area detector and a graphite monochromator. The temperature used was 295 K. Cell parameters were refined using 2245 reflections for $Ag_2(C_5H_3N_2O_4)_2 \cdot 2H_2O$, 1040 for $KC_5H_3N_2O_4$ and 2244 for $RbC_5H_5N_2O_4$. A hemisphere of data (1291 frames) was collected for each structure using the ω-scan method (0.3° frame width) with a crystal–detector distance of 5.0 cm. The first 50 frames were remeasured at the end of the data collection to monitor instrument and crystal stability. Intensity decay was negligible for all three crystals. All reflections were merged and integrated using SAINT and empirical absorption corrections were applied using SADABS.[28] The structures were solved by direct methods in SHELXTL and refined using full-matrix least squares on F^2. Non-H atoms were treated anisotropically. Hydrogen atoms were located by difference Fourier maps but refined with the distances constrained to 0.86 (N–H) and 0.97 Å (C–H). The crystal data and details of the data collection and refinement are given in Table 1.

CCDC reference numbers 174142–174144.

See http://www.rsc.org/suppdata/dt/b1/b110386p/ for crystallographic data in CIF or other electronic format.

Table 1 Crystallographic data

	1	2	3
Formula	$Ag_2(C_5H_3O_4N_2)_2 \cdot 2H_2O$	$KC_5H_3O_4N_2$	$RbC_5H_3O_4N_2$
M/g mol^{-1}	560.95	194.19	240.56
T/K	295	295	295
Crystal system	Triclinic	Orthorhombic	Orthorhombic
Space group	$P\bar{1}$ (no. 2)	*Cmma* (no. 67)	*Cmma* (no. 67)
a/Å	5.1295(5)	6.834(3)	7.2007(10)
b/Å	5.9118(6)	12.565(6)	12.7622(18)
c/Å	12.1815(12)	7.668(4)	7.7583(11)
α/°		92.071(2)	90.00 90.00
β/°	96.540(2)	90.00	90.00
γ/°	106.322(2)	90.00	90.00
V/Å^3	351.30(6)	658.5(5)	712.96(17)
Z	1	4	4
μ/cm^{-1}	2.859	0.777	6.917
Reflections measured	2175	1541	2234
Unique reflections (R_{int})	1434 (0.0175)	370 (0.0226)	483 (0.0277)
Observed reflections, $I > 2\sigma(I)$	1199	251	385
R_1 (observed reflections)	0.0313	0.0794	0.0262
wR_2 (all reflections)	0.0720	0.2616	0.0681
$\Delta\rho_{min}$, $\Delta\rho_{max}$/e Å^{-3}	−0.754, 0.751	−0.805, 0.995	−0.507, 0.375

Computational methods

All calculations were performed at the *ab initio* level using the Gaussian-98 computer code.[23] Geometries and vibrational frequencies in the harmonic approximation were computed at the B3LYP/6-31G(d) level. In all calculations, the TIGHT keyword calling for more restricted convergence was used and the wavefunctions were verified to be stable using the STABLE keyword. Two sets of NMR calculations were performed on the optimized structures using HF/6-311++G(2d,2p) and B3LYP/6-311++G(2d,2p) model chemistries to check the computational robustness, since DFT NMR calculations use functionals where intrinsic parameters for magnetic filed susceptibilities are not involved. The NMR magnetic shielding tensor for TMS protons and carbon are 31.6297 and 182.4572 ppm for B3LYP/6-311++G(2d,2p) and 31.8927 and 192.8847 ppm for HF/6-311++G(2d,2p), respectively, and the isotropic shieldings of ^{1}H and ^{13}C were converted to chemical shifts by taking the difference of the TMS values.

Acknowledgements

We are grateful to Dr Corine Sandström for recording and discussing the NMR spectra.

References

1 D. Shugar and J. J. Fox, *Biochim. Biophys. Acta.*, 1952, **9**, 199.
2 D. J. Darensbourgh, D. L. Larkins and J. H. Reibenspeiss, *Inorg. Chem.*, 1998, **37**, 6125.
3 T. W. Hambley, R. I. Christopherson and E. S. Zvargulis, *Inorg. Chem.*, 1995, **34**, 6550; N. Lalioti, C. P. Raptopoulou, A. Terzis, A. Panagiotopoulos, S. P. Perlepes and E. Manessi-Zoupa, *J. Chem. Soc., Dalton Trans.*, 1998, 1327.
4 D. Mentzafos, N. Katzaros and A. Terzis, *Acta Crystallogr., Sect. C*, 1987, **43**, 1905.
5 O. Kumberger, J. Riede and H. Schmidbaur, *Z. Naturforsch., Teil B*, 1993, **48**, 961.
6 I. Bach, O. Kumberger and H. Schmidbaur, *Chem. Ber.*, 1990, **123**, 2267.
7 I. Mutikainen and P. Lumme, *Acta Crystallogr., Sect. B*, 1980, **36**, 2233; T. S. Khodashova, M. A. Porai-Koshits, N. K. Davidenko and N. N. Vlasova, *Koord. Khim.*, 1984, **10**, 262.
8 A. Karipides and B. Thomas, *Acta Crystallogr., Sect. C*, 1986, **42**, 1705.
9 T. Solin, K. Matsumoto and K. Fuwa, *Bull. Chem. Soc. Jpn.*, 1981, **54**, 3731.
10 A. D. Burrows, D. M. P. Mingos, A. J. P. White and D. J. Williams, *J. Chem. Soc., Dalton Trans.*, 1996, 3805.
11 P. Castan, T. Ha, F. Nepveu and G. Bernardinelli, *Inorg. Chim. Acta*, 1995, **221**, 173.
12 S. L. James, D. M. P. Mingos, X. Xu, A. J. P. White and D. J. Williams, *J. Chem. Soc., Dalton Trans.*, 1998, 1335.
13 D. J. Darensbourg, J. D. Draper, D. J. Larkins, B. J. Frost and J. H. Reibenspeis, *Inorg. Chem.*, 1998, **37**, 2538.
14 F. Nepveu, N. Gaultier, N. Korber, J. Jaud and P. Castan, *J. Chem. Soc., Dalton Trans.*, 1995, 4005.
15 P. Arrizabalaga, P. Castan and F. Dahan, *Inorg. Chem.*, 1983, **22**, 2245.
16 C. P. Raptopoulou, V. Tangoulis and V. Psycharis, *Inorg. Chem.*, 2000, **39**, 4452.
17 *e.g.* G. Smith, A. N. Reddy, K. A. Byriel and C. H. L. Kennard, *Polyhedron*, 1994, **13**, 2425; P. Pingrong Wei, T. C. W. Mak and D. A. Atwood, *Inorg. Chem.*, 1998, **37**, 2605; F. Jaber, F. Charbonnier and R. Faure, *Polyhedron*, 1996, **15**, 2909; K. Nomiya, S. Takahashi and R. Noguchi, *J. Chem. Soc., Dalton Trans.*, 2000, 1343 and references therein.
18 R. Kiralj, G. Kojic-Prodic, I. Piantanida and M. Zinic, *Acta Crystallogr., Sect. B*, 1999, **55**, 55.
19 C. B. Aakeröy, A. M. Beatty and D. S. Leinen, *J. Am. Chem. Soc.*, 1998, **120**, 7383.
20 J. Solbakk, *Acta Chem. Scand.*, 1971, **25**, 3006.
21 R. D. Shannon, *Acta Crystallogr., Sect. A*, 1976, **32**, 751; R. D. Shannon and C. T. Prewitt, *Acta Crystallogr., Sect. B*, 1969, **25**, 925; R. D. Shannon and C. T. Prewitt, *Acta Crystallogr., Sect. B*, 1970, **26**, 1046.
22 D. Becke, *J. Chem. Phys.*, 1993, **98**, 5648.
23 Gaussian-98 (Revision A.3), M. J. Frisch, G. W. Trucks, H. B. Schlegel, G. E. Scuseria, M. A. Robb, J. R. Cheeseman, V. G. Zakrzewski, J. A. Montgomery, R. E. Stratmann, J. C. Burant, S. Dapprich, J. M. Millam, A. D. Daniels, K. N. Kudin, M. C. Strain, O. Farkas, J. Tomasi, V. Barone, M. Cossi, R. Cammi, B. Mennucci, C. Pomelli, C. Adamo, S. Clifford, J. Ochterski, G. A. Petersson, P. Y. Ayala, Q. Cui, K. Morokuma, D. K. Malick, A. D. Rabuck, K. Raghavachari, J. B. Foresman, J. Cioslowski, J. V. Ortiz, B. B. Stefanov, G. Liu, A. Liashenko, P. Piskorz, I. Komaromi, R. Gomperts, R. L. Martin, D. J. Fox, T. Keith, M. Al-Laham, C. Y. Peng, A. Nanayakkara, C. Gonzalez, M. Challacombe, P. M. W. Gill, B. G. Johnson, W. Chen, M. W. Wong, J. L. Andres, M. Head-Gordon, E. S. Replogle and J. A. Pople, Gaussian, Inc., Pittsburgh, PA, 1998.
24 F. Takusagawa and A. Shimada, *Bull. Chem. Soc. Jpn.*, 1973, **46**, 201.
25 D. A. Singleton, S. R. Merrigan, B. J. Kim, P. Beak, L. M. Phillips and J. K. Lee, *J. Am. Chem. Soc.*, 2000, **122**, 3296.
26 J. R. Cheeseman, G. W. Trucks, T. A. Keith and M. J. Frisch, *J. Chem. Phys.*, 1996, **104**, 5497.
27 A. Hernanz, F. Billes, I. Bratu and R. Navarro, *Biopolym. (Biospectrosc.)*, 2000, **57**, 187.
28 SHELXTL (v. 5.1), SADABS and SAINT (v. 5.01), Bruker Analytical X-ray Systems, Madison, Wisconsin, USA.